JAIST Repository
https://dspace.jaist.ac.jp/

Title	High-In-content InGaAs quantum point contacts fabricated using focused ion beam system equipped with N_2 gas field ion source
Author(s)	Akabori, Masashi; Hidaka, Shiro; Yamada, Syoji; Kozakai, Tomokazu; Matsuda, Osamu; Yasaka, Anto
Citation	Japanese Journal of Applied Physics, 53(11): 118002-1-118002-3
Issue Date	2014-10-09
Type	Journal Article
Text version	author
URL	http://hdl.handle.net/10119/12316
Rights	This is the author's version of the work. It is posted here by permission of The Japan Society of Applied Physics. Copyright (C) 2014 The Japan Society of Applied Physics. Masashi Akabori, Shiro Hidaka, Syoji Yamada, Tomokazu Kozakai, Osamu Matsuda and Anto Yasaka, Japanese Journal of Applied Physics, 53(11), 2014, 118002-1-118002-3. http://dx.doi.org/10.7567/JJAP.53.118002
Description	

JAIST
JAPAN ADVANCED INSTITUTE OF SCIENCE AND TECHNOLOGY

Japan Advanced Institute of Science and Technology

High-In-content InGaAs quantum point contacts fabricated using focused ion beam system equipped with N_2 gas field ion source

Masashi Akabori[1, *], Shiro Hidaka[1], Syoji Yamada[1], Tomokazu Kozakai[2], Osamu Matsuda[2], and Anto Yasaka[2]

[1] *Center for Nano Materials and Technology (CNMT), Japan Advanced Institute of Science and Technology (JAIST), Nomi, Ishikawa 923-1292, Japan*

[2] *Hitachi High-Tech Science Corporation, Oyama, Shizuoka 410-1393, Japan*

[*]E-mail: akabori@jaist.ac.jp

Quantum point contacts (QPCs) in high-In-content InGaAs modulation-doped heterostructures fabricated using a focused ion beam (FIB) system equipped with a N_2 gas field ion source (GFIS) are demonstrated. The minimum physical size of the fabricated QPC structures in this study is ~30 nm, which is smaller than the typical physical size of QPCs (> 50 nm) obtained by electron beam lithography and etching techniques. In addition, the fabricated QPCs are characterized electrically at low temperatures with magnetic fields. Since some of them show conductance quantization behaviors, the results indicate that the GFIS-FIB process is promising for quantum device fabrication.

Modulation-doped heterostructures (MDHs) including high-In-content InGaAs have been expected to be applied to spintronic quantum devices, because they show high electron mobility, large g-factor, and strong Rashba-type spin-orbit coupling (SOC), which can be controlled by external electric fields.[1-3] Quantum point contacts (QPCs) are typical quantum nanostructures, which can be applied to spintronic quantum devices.[4-5] Indeed, QPCs made from InGaAs MDHs have been intensively studied, [6-12] and some of them have focused on spin polarizers[7, 10] and Stern-Gerlach spin splitters.[12] These QPCs have been fabricated by electron beam lithography and etching techniques; however, the achievable physical size of the structures is ~50 nm.

A gas field ion source (GFIS) ionizes gas molecules in a high electrical field on an atomically sharp tip-like field ion microscope,[13] creating a beam of charged particles; thus, it can be used as a source of focused ion beams (FIBs). Since the GFIS has a smaller beam spot than a typical Ga liquid metal ion source, GFIS-FIB is more suitable for fine patterning than Ga-FIB. A conventional GFIS-FIB system uses an ionized He beam, and it is called a helium ion microscope (HIM).[14] HIM has been used for the direct fine patterning of graphene;[15-16] however, the low mass of He is not suitable for deep patterning. To realize the deep patterning, we have chosen N_2 for GFIS-FIB, which is, to the best of our knowledge, the first attempt in the world. The minimum line width realized by physical sputtering using an ionized N_2 beam is 10 nm or even smaller with a depth of ~50 nm.[17] On the other hand, Ga-FIB has also been used for the fabrication of QPCs made from GaAs[18] and InGaAs MDHs.[19] Therefore, if N_2 GFIS-FIB is used for the fabrication of QPCs, there is a possibility of realizing QPCs with a physical size < 50 nm, which is difficult to obtain by electron beam lithography and etching techniques.

In this study, we employed N_2 GFIS-FIB to form QPCs in an inverted high-In-content InGaAs

MDH[20-21] by physical sputtering. To control QPCs electrically, we formed top-gate structures by atomic layer deposition (ALD) of Al_2O_3 followed by Ti/Au evaporation and lift-off after GFIS-FIB fine patterning. We also carried out electrical measurements of the fabricated QPC structures at low temperatures to confirm their operations.

The inverted high-In-content InGaAs MDH was grown on a semi-insulating GaAs (001) substrate by molecular beam epitaxy with InAlAs step-graded buffers (SGBs).[20-21] The MDH consists of a 60-nm-thick InGaAs channel (top), a 20-nm-thick InAlAs spacer, a Si delta-doping layer, a 200-nm-thick InAlAs barrier, and InAlAs SGBs (bottom). The nominal In content is 0.75 for active layers (channel, spacer, and barrier). For QPC fabrication, we first formed Hall bar mesas by conventional photolithography and wet chemical etching. Then, we carried out photolithography, AuGeNi evaporation, lift-off, and annealing for ohmic electrodes of Hall bars. After the Hall bar fabrication, some samples were wet-chemically etched to reduce the InGaAs thickness to 40 nm. Then, we fabricated μm-size constrictions at the center of the Hall bars using Ga-FIB or the combination of photolithography and wet chemical etching. After the fabrication of μm-size constrictions, we loaded the samples into a GFIS-FIB fine patterning machine. With imaging by ionized N_2 beam scanning, we found out the μm-size constrictions, and then we formed QPCs by physical sputtering of an ionized N_2 beam. The nominal depth of the physical sputtering is ~200 nm, and the process time for the QPCs formed is ~10–15 min. Figure 1 shows scanning electron microscopy images of the QPC after GFIS-FIB fine patterning. The length and width of the QPC are ~30 and ~100 nm, respectively. These results indicate that GFIS-FIB enables us to perform fine patterning (~ 30 nm) for compound semiconductors such as InGaAs MDHs. After GFIS-FIB fine patterning, we carried out ALD of Al_2O_3 with trimethylaluminum and water. The thickness of Al_2O_3 is ~30 nm. The post-deposition annealing was carried out at 350 °C for 30 min in Ar/H_2(10 %) ambient. Finally, we formed the top gate by photolithography, Ti/Au evaporation, and lift-off. For electrical

measurements, we used a ^{4}He cryostat with a superconducting magnet and a standard AC lock-in technique with AC voltage excitation (V_D: 0.1-100 mV peak-to-peak) and a current preamplifier.

First, we carried out electrical measurements of QPCs without the wet chemical surface etching of Hall bars. Figure 2 shows the conductance G curve of a QPC with a 60-nm-thick InGaAs channel as a function of the gate voltage V_G. The conductance G was calculated by measuring drain current and the root mean square of AC voltage excitation. The length and width of the QPC are 70 and 200 nm, respectively. Despite the application of a negative gate voltage, the reduction in conductance seems small (~ 0.3 x $2e^2/h$) at $-9\ \mathrm{V} < V_G < 0\ \mathrm{V}$. Moreover, the increase in conductance at approximately $V_G < -9$ V can be seen. Since the gate current in the QPC is < 100 times lower than the drain current, the increase does not originate from the leakage. In addition, another QPC with the same 60-nm-thick channel and a smaller constriction (30 nm length and 100 nm width) showed a smaller conductance (~ 0.5 x $2e^2/h$) but a similar increase behavior. Thus, the smaller constriction does not help in enhancing gate controllability, and it seems difficult to achieve the pinch-off of QPCs as well as quantized conductance steps in the case of the 60-nm-thick channel. This may originate from the generation of the inversion layer at the Al_2O_3/InGaAs interface after the application of a high negative gate voltage due to the narrow bandgap of the thick InGaAs.

Next, we carried out electrical measurements of QPCs with the wet chemical surface etching of Hall bars. Figure 3 shows the conductance G and numerically derived dG/dV_G curves of a QPC with a 40-nm-thick InGaAs channel as a function of the gate voltage V_G. In this case, the conductance becomes almost zero when the gate voltage is approximately $V_G \sim 0$ V. Therefore, the generation of the surface inversion layer seems to be suppressed owing to the small channel thickness, and the pinch-off of the QPC seems to be almost realized. Moreover, dip structures

in the derived curves, which correspond to step-like structures in the conductance curves, can be seen at approximately the quantized conductance value (~ $2e^2/h$). Thus, this result can be considered as conductance quantization and suggests that the QPCs fabricated using N_2 GFIS-FIB can work as quantum devices. However, the half-integer quantized conductance (0.5 x $2e^2/h = e^2/h$), which is expected to appear in the case of strong SOC,[7, 10, 12)] could not be observed. Since similar InGaAs MDHs experimentally show strong Rashba SOC (~10^{-11}-10^{-12} eVm),[20-22)] ionized N_2 beam irradiation during imaging and/or sputtering in the GFIS-FIB process may reduce the sheet electron concentration locally and weaken the SOC owing to the reduction in effective electric field. Also, the conductance seems saturated less than twice the quantized conductance (2 x $2e^2/h$). Since the physical width of this QPC structure is ~150 nm and the length is sufficient compared with a typical Fermi wavelength, the result also implies that the beam irradiation affects electrical conduction properties such as reductions in sheet electron concentration and electron mobility. Since we did not control the beam irradiations in the present experiments, we could not quantitatively evaluate the negative effect of damage caused by the beam irradiation. In the future, we will control the beam irradiations and evaluate the irradiation-induced damage through electrical properties.

To investigate the conductance quantization in more detail, we carried out electrical measurements of QPCs in magnetic fields. Figure 4 shows the G and numerically derived dG/dV_G curves of another QPC with a 40-nm-thick InGaAs channel under various magnetic fields as a function of the gate voltage. With increasing magnetic field, the conductance of 1st step-like structures at V_G ~ 0.8 V seems reduced from ~$2e^2/h$ to ~0.5 x $2e^2/h$ (= e^2/h). In addition, the conductance of 2nd step-like structures at V_G ~ 2.5 V seems also reduced from ~2 x $2e^2/h$ (= $4e^2/h$) to ~1.5 x $2e^2/h$ (= $3e^2/h$). These results can be understood by considering Zeeman spin splitting, and provide evidence of the QPC operation. However, we note that there seem no step-like structures of ~$2e^2/h$ at $0.8 \text{ V} < V_G < 2.5 \text{ V}$ under high magnetic fields. This behavior

is unexpected, but we have no idea on how to explain this at the moment.

In summary, we fabricated QPC structures in inverted high-In-content InGaAs MDHs by physical sputtering using N_2 GFIS-FIB. The minimum length of the QPC structures is ~30 nm, which is smaller than the size achievable by electron beam lithography and etching techniques. We also carried out electrical measurements of the fabricated QPC structures at low temperatures. We confirmed that the QPC structures with a 40-nm-thick InGaAs channel show step-like structures in the conductance curves, which correspond to the quantized conductance ($2e^2/h$). In addition, we confirmed half-integer quantized conductance behaviors (e^2/h and $3e^2/h$) under magnetic fields. These results indicate that the GFIS-FIB process is promising for quantum device fabrication.

REFERENCES

1) J. Nitta, T. Akazaki, H. Takayanagi, and T. Enoki, Phys. Rev. Lett. **78**, 1335 (1997).

2) Th. Schäpers, G. Engels, J. Lange, Th. Klocke, M. Hollfelder, and H. Lüth, J. Appl. Phys. **83**, 4324 (1998).

3) Y. Sato, T. Kita, S. Gozu, and S. Yamada, J. Appl. Phys. **89**, 8017 (2001).

4) M. Eto, T. Hayashi, and Y. Kurotani, J. Phys. Soc. Jpn. **74**, 1934 (2005).

5) M. Eto, T. Hayashi, Y. Kurotani, and H. Yokouchi, Phys. Status Solidi C **3**, 4168 (2006).

6) M. F. Tietze, Th. Schäpers, J. Appenzeller, G. Engels, M. Hollfelder, B. Lengeler, and H. Lüth, J. Appl. Phys. **79**, 871 (1996).

7) T. Kita, T. Kakegawa, M. Akabori, and S. Yamada, Physica E **22**, 464 (2004).

8) Th. Schäpers, V. A. Guzenko, and H. Hardtdegen, Appl. Phys. Lett. **90**, 122107 (2007).

9) T. P. Martin, C. A. Marlow, L. Samuelson, A. R. Hamilton, H. Linke, and R. P. Taylor, Phys. Rev. B **77**, 155309 (2008).

10) P. Debray, S. M. S. Rahman, J. Wan, R. S. Newrock, M. Cahay, A. T. Ngo, S. E. Ulloa, S. T. Herbert, M. Muhammad, and M. Johnson, Nat. Nanotechnol. **4**, 759 (2009).

11) H. Irie, Y. Harada, H. Sugiyama, and T. Akazaki, Appl. Phys. Express **5**, 024001 (2012).

12) M. Kohda, S. Nakamura, Y. Nishihara, K. Kobayashi, T. Ono, J. Ohe, Y. Tokura, T. Mineno, and J. Nitta, Nat. Commun. **3**, 1082 (2012).

13) E. W. Müller, Z. Phys. **131**, 136 (1951) [in German].

14) B. W. Ward, J. A. Notte, and N. P. Economou, J. Vac. Sci. Technol. B **24**, 2871 (2006).

15) D. C. Bell, M. C. Lemme, L. A. Stern, J. R. Williams, and C. M. Marcus, Nanotechnology **20**, 455301 (2009).

16) S. A. Boden, Z. Moktadir, D. M. Bagnall, H. Mizuta, and H. N. Rutt, Microelectron. Eng. **88**, 2452 (2011).

17) F. Aramaki, T. Kozakai, O. Matsuda , O. Takaoka, Y. Sugiyama, H. Oba, K. Aita, and A. Yasaka, Proc. SPIE **8441**, 84410D (2012).

18) Y. Hirayama, A. D. Wieck, and K. Ploog, J. Appl. Phys. **72**, 3022 (1992).

19) T. Bever, Y. Hirayama, and S. Tarucha, Jpn. J. Appl. Phys. **33**, L800 (1994).

20) H. Choi, T. Kakegawa, M. Akabori, T. Suzuki, and S. Yamada, Physica E **40**, 2823 (2008).

21) S. Nitta, H. Choi, and S. Yamada, Physica E **42**, 987 (2010).

22) S. Hidaka, M. Akabori, and S. Yamada, Appl. Phys. Express **5**, 113001 (2012).

FIGURE CAPTIONS

Fig. 1. (Color online) Scanning electron microscopy images of a QPC fabricated using N_2 GFIS-FIB. The images were taken immediately after the GFIS-FIB patterning process before the top-gate formation.

Fig. 2. (Color online) Conductance curve of a QPC with a 60-nm-thick InGaAs channel as a function of the gate voltage. The length and width of the QPC are 70 and 200 nm, respectively.

Fig. 3. (Color online) Conductance and numerically derived curves of a QPC with a 40-nm-thick InGaAs channel as a function of the gate voltage for various AC voltage excitations. The curve offset is $2e^2/h$. The length and width of the QPC are 30 and 150 nm, respectively. The blue broken line represents the position of the 1st quantized conductance step.

Fig. 4. (Color online) Conductance and numerically derived curves of another QPC with a 40-nm-thick InGaAs channel as a function of the gate voltage for various magnetic fields. The curve offset is $2e^2/h$. The length and width of the QPC are 30 and 150 nm, respectively. Arrows represent the positions of the 1st and 2nd quantized conductance steps.

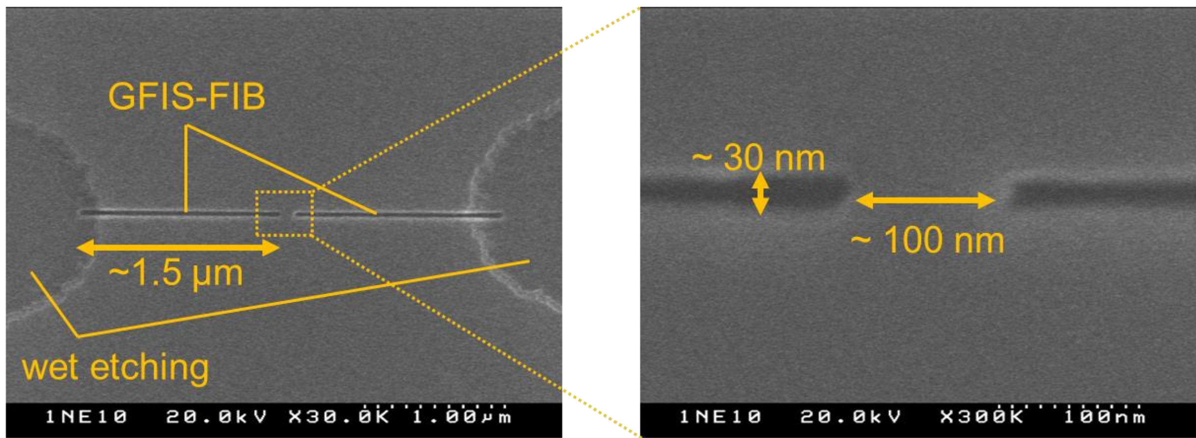

Figure 1

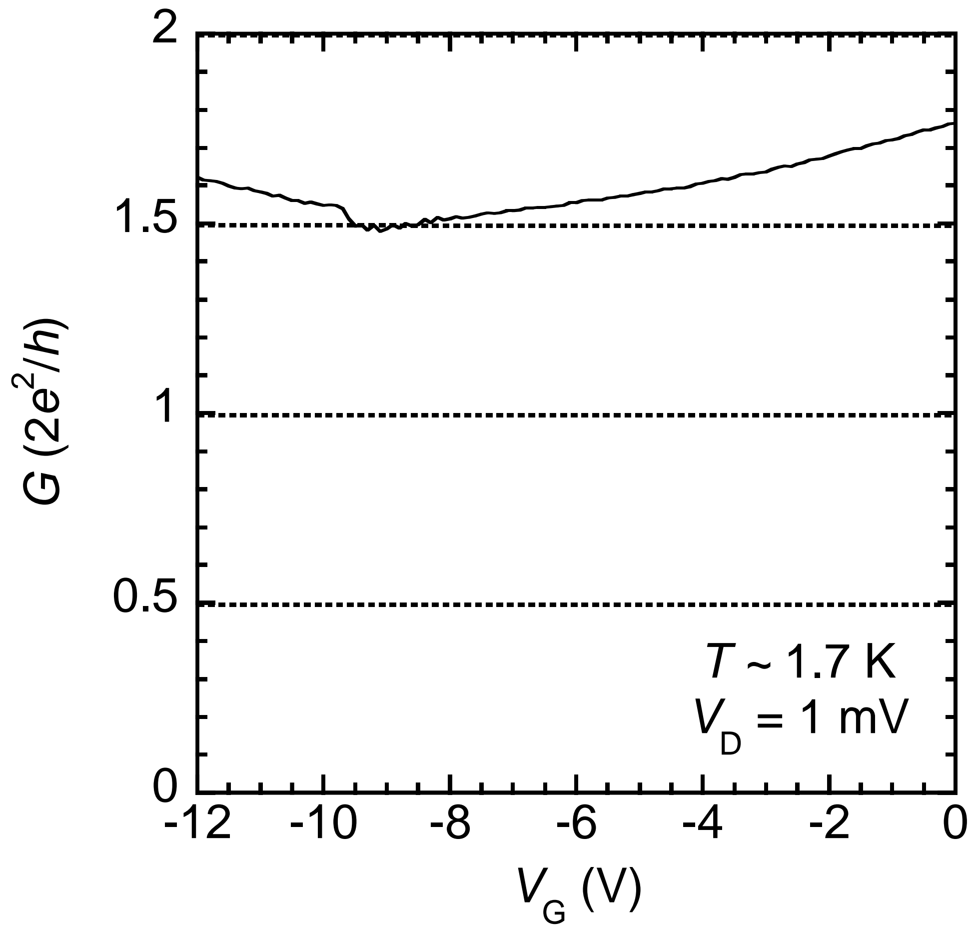

Figure 2.

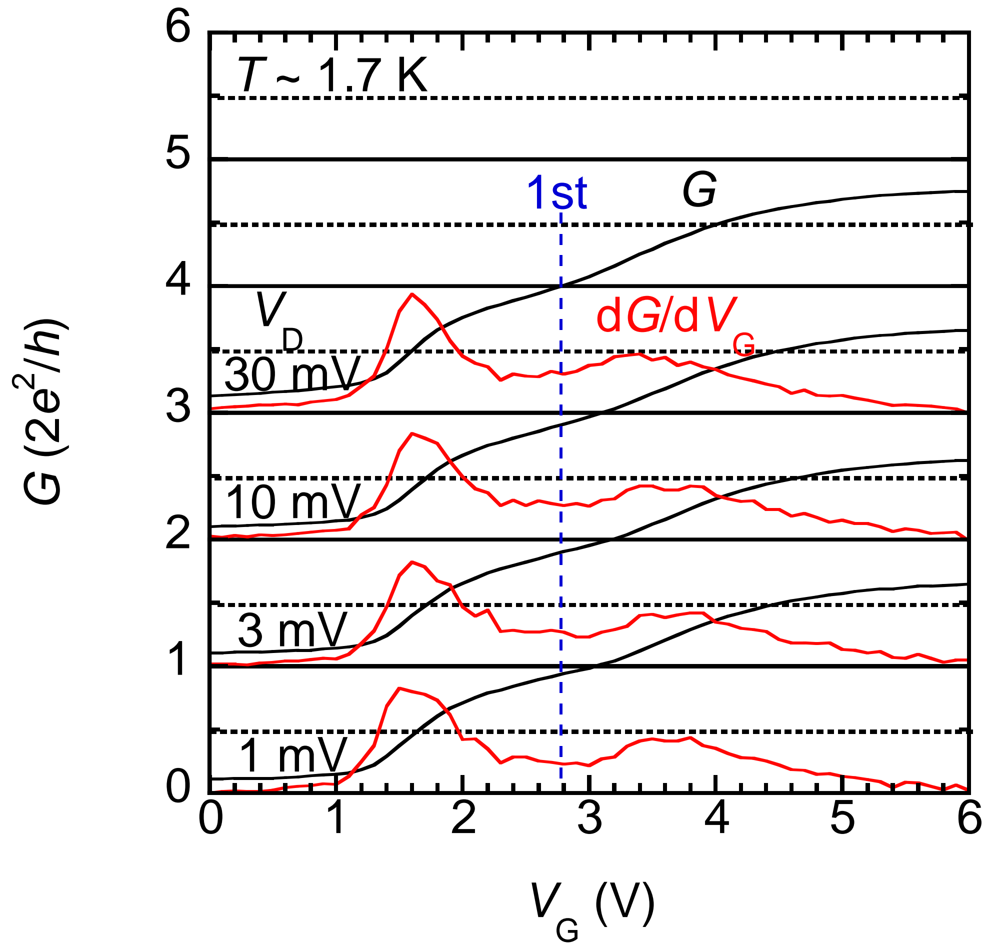

Figure 3.

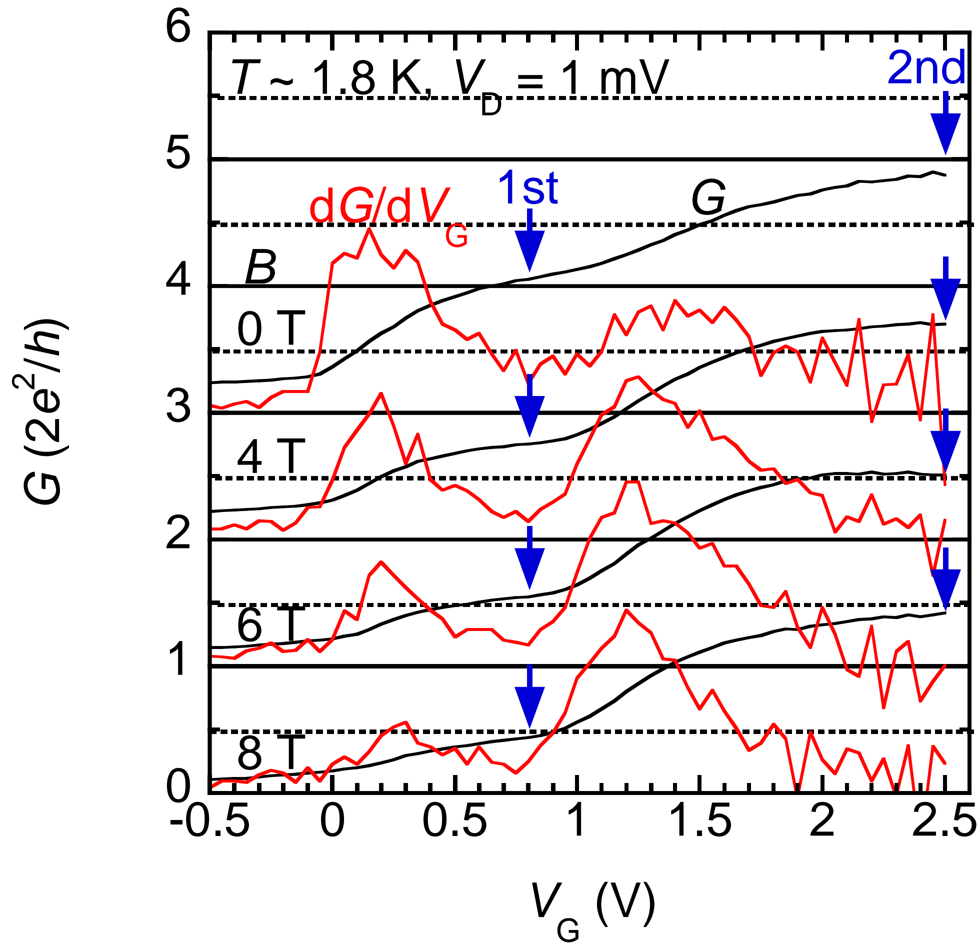

Figure 4.